Calculated sheath dynamics under the influence of an asymmetrically pulsed dc bias

E. V. Barnat and T.-M. Lu
Department of Physics, Applied Physics, and Astronomy, and the Center for Integrated Electronics, Rensselaer Polytechnic Institute, Troy, New York 12180-3590
(Received 20 May 2002; published 5 November 2002)

A one-dimensional model is used to describe the evolution of charged particles in a plasma sheath driven by an asymmetrically pulsed dc bias in the frequency range of 100 kHz to 10 MHz. The temporal-spatial evolution of the sheath is obtained through the simultaneous solution of Poisson's equations, the ionic fluid equations and a Boltzmann treatment of the electrons. Calculations are performed to demonstrate the effects ionic inertia and sheath restructuring have on the temporal dependence of current and energy of the ions arriving at the driven electrode. The temporal scale is observed to depend on the bulk density of the plasma. The pulse frequency, the pulse duty, and the capacitive coupling of the pulse to the driving electrode are varied to demonstrate the influence of these factors on the energy distribution of the ions extracted from the plasma to the electrode.

DOI: 10.1103/PhysRevE.66.056401 PACS number(s): 52.40.Kh, 52.65.Cc, 52.65.Rr

I. INTRODUCTION

Plasma based systems are used extensively for the modification of materials. The flux of charged particles from these plasmas are typically responsible for the interactions that govern the modifying processes. For example, both the energy and the number of charged particles impacts the depth and concentration of implanted species and can modify the electrical [1] or mechanical [2] properties of a material. Energies of ion extracted from a plasma can also influence the etch rate and selectivity of the etched material [3,4]. During plasma based vapor deposition, such as sputtering, the energy of the ions can influence the nature of microstructural evolution of thin films being grown [5,6].

In typical plasma based processing, an electrical bias is applied to the electrode exposed to the plasma to control the extraction of charge. When a dc bias cannot be employed, because of the nature of the material being processed or coupling of the electrode to the power supply, a radio frequency (rf) bias is typically used. It is well documented that the energy spectrum of the ions extracted from the plasma by an rf powered electrode is bimodal in nature [7,8]. Several studies related the shape of the spectrum, including peak widths and intensities, as being governed by the time scales of the ionic response to the applied rf fields [9–12]. The energy spectrum was broad at low frequencies because the ions respond instantaneously to the rf field and converged as the time scales of the rf period became greater than the time scales of the ion transit time and the ion responds to the time averaged rf field.

A series of previous articles had discussed the topic of asymmetrically pulse biasing a substrate for the control of charge accumulation and ultimately the control of the flux of ions extracted from the plasma [13–15]. Asymmetrical pulsing was described as offering a unique alternative to standard rf techniques through the ability to control the energy distribution of the ions extracted from the plasma by varying not only the amplitude and the frequency, but the duty of the pulse as well. The duty of the pulse (defined as the ratio of time the pulse is in the electrically biased low state, to the total period of the pulse) was adjusted to introduce asymmetry in the pulse to capitalize on the asymmetry of the ionic and electronic response to the applied fields. This asymmetry ultimately led to the control of the energy spectrum of the ions extracted from the plasma [5,15].

In the mentioned studies [5–15], the sheath was assumed to be quasistatic and the ions were assumed to respond instantaneously to the transient potentials of the driving electrode. The validity of these approximations was discussed in terms of the limitations placed on the time scales of the pulse period. Limiting time scales were expressed in terms of the ionic response time and the ratio of displacement currents to total ionic currents to the electrode [14,15]. These limiting time scales were functionally dependant on the plasma density and pulse amplitude. For typical conditions of interest, the limiting time scales are on the order of one microsecond, corresponding to critical frequencies of 1 MHz.

In this study, we employ numerical calculations to describe the response of the ions to a pulsed electrode when the time scales of interest make previous approximations invalid. The time scales examined in this study correspond to pulse frequencies in the range of 100 kHz–10 MHz. The treatment of the charge in the sheath, as initially suggested by Widner, Alexeff, and Jones [16] and subsequently used by Emmert [17] is employed to predict the effect of the transient potentials in the sheath on the ionic flux to an asymmetrically driven electrode. This treatment assumes that the electrons respond instantaneously to changes in the potential (electronic response time to transient fields are much smaller than the times scales of interest) and the spatial electron density is described by the Boltzmann distribution. Spatial and temporal responses of the ions to changes in the potential are obtained through the solution of the one-dimensional ion fluid equations. Poisson's equation is used to solve for the potential in terms of the ion and electron densities. The temporal and spatial evolution of the sheath's potential is obtained to demonstrate the transient nature of the sheath under the influence of a pulsed bias to the electrode. Energies and currents of the ions to the electrode are examined as functions of time to illustrate the effect of the ionic inertia and the sheath

restructuring have on the ionic fluxes. In discussing the energies and currents of the ions, we examine the factors that ultimately influence the final energy distribution of the ions extracted from the sheath. These factors include the plasma density, the shape of the applied pulse (the asymmetry of the pulse and the frequency of the pulse), and the capacitive coupling of the pulse to the driving electrode.

II. SHEATH MODEL

As mentioned in the Introduction, the model used to predict the evolution of the sheath was introduced by Widner, Alexeff, and Jones [16] and employed by Emmert [17]. The one-dimensional equations and the procedures to obtain their solutions are the same as those employed by Emmert. We briefly describe the equations and the methods used to solve these equations for completeness.

The evaluation space is bound by the driven electrode at $x=0$ and the ''bulk'' plasma at $x=x_s$, where x_s is given by

$$x_s = N\lambda_{Debye} = N\sqrt{\frac{\varepsilon_0 kT_e}{e^2 n_0}}, \tag{1}$$

where N is a number that establishes the width of the evaluation in terms of λ_{Debye}, the Debye length. ε_0 is the permittivity of free space, kT_e is the electron temperature, e is the elementary charge and n_o is the ionic and electronic density of the bulk plasma. For the calculations presented in this study kT_e is assumed to be 2 eV and N is set to 30 to ensure that sufficient space is provided to shield the bulk plasma from the fields induced by the electrode's bias.

The evaluation space is divided into evenly spaced cells, the reference cells, which are bound by reference points. These reference points, and in turn the width of the reference cells, remain fixed for the calculations. Each reference cell is subsequently subdivided into cells, tracer cells, which are bound by tracer ions. Tracer ion i represents the average ion density and velocity of the tracer cell i as bound by tracer ion i and tracer ion $i+I$. Initially, each tracer ion of mass m_i, is assigned the bulk density, n_0, and an initial drift velocity, $-u_{Bohm}$ $[=(kT_e/m_i)^{1/2}]$, the Bohm velocity. The Bohm drift condition is imposed to ensure a constant flux of ions from the plasma to the sheath region and can be considered as being caused by an acceleration from some presheath region (not treated here). The direction of the drift is from the plasma $x=x_s$ to the electrode $x=0$. For our discussion, we divide the evaluation space into 180 reference cells and initially begin with 1800 tracer ions (subdivide each reference cell by 10).

To obtain the evolution of the sheath under the applied potential to the electrode, we begin with Poisson's equation relating the charge to the electrical potential,

$$\frac{\partial^2 \Phi(x,t)}{\partial x^2} = -\frac{e}{\varepsilon_0}[n_i(x,t) - n_e(x,t)], \tag{2}$$

where $\Phi(x,t)$ is the potential at position x, at time t, and n_x is the ionic and electronic densities at position x, and at time t. The ion densities n_i are assigned to each of the jth reference point through extrapolation of the ith tracer cells that are in the spatial domain bound by the reference cells $j-I$ and $j+I$. The interpolation of the charge to the reference point j is done by a linear weighing technique over the tracer cells in the domain of interest [18]. The electron densities are given by the Boltzmann relation as given by

$$n_e = n_0 e^{\Phi/kT_e}. \tag{3}$$

Two boundary conditions are required to solve the Poisson's equation. The first boundary condition is $\Phi(x_s,t) = \text{constant} \equiv 0$, defining the bulk plasma potential. The second condition is placed on the electrode's potential at $x=0$. Here, the electrode is driven by an asymmetrically driven pulsed bias as prescribed by

$$\Phi(0,t) = eV_{Electrode} = A_0 + \sum_{n=1}^{N} A_n \sin(n\omega t) + \sum_{n=1}^{N} B_n \cos(n\omega t), \tag{4a}$$

a Fourier series, where ω is the angular frequency of the applied pulse of frequency ν, and A_n and B_n are the Fourier coefficients as prescribed by

$$A_0 = \frac{e}{\tau}[V_{Low}\tau_{Low} + V_{High}\tau_{High}], \tag{4b}$$

$$A_n = \frac{e}{n\pi}\left\{ V_{Low}\left[\cos\left(2n\pi \frac{\tau_{Low}}{\tau} \right) - 1 \right] + V_{High}\left[1 - \cos\left(2n\pi \frac{\tau_{Low}}{\tau} \right) \right] \right\}, \quad n \geq 1, \tag{4c}$$

$$B_n = \frac{e}{n\pi}[V_{Low} - V_{High}] \sin\left(2n\pi \frac{\tau_{Low}}{\tau} \right), \quad n \geq 1. \tag{4d}$$

V_{Low} and V_{High} are the electrical potentials the electrode is pulsed between ($V_{Low} < V_{High}$), τ is the pulse period ($1/\nu$), and τ_{Low} and τ_{High} are the times that the pulse is in the low and high states ($\tau = \tau_{Low} + \tau_{High}$). As described in more detail by Emmert, Poisson's equation, (2), is then scaled and iteratively solved by linearizing Poisson's equation and using a finite differencing technique. The Thomas algorithm [19] was the specific technique used to carry out the finite differencing procedure. When the obtained potential profile was within $0.1kT_e$ (0.2 V) of the potential profile of previous iteration, the iterative process was ended and the spatial potential for each reference point for a given time t was obtained. The potential and the electric fields, as obtained by the spatial derivative of the potential, were then interpolated for each of the tracer ions.

The collisionless ionic equations of motion,

$$m_i \frac{\partial u_i}{\partial t} + m_i u_i \frac{\partial u_i}{\partial x} = -e\frac{\partial \Phi}{\partial x}, \tag{5a}$$

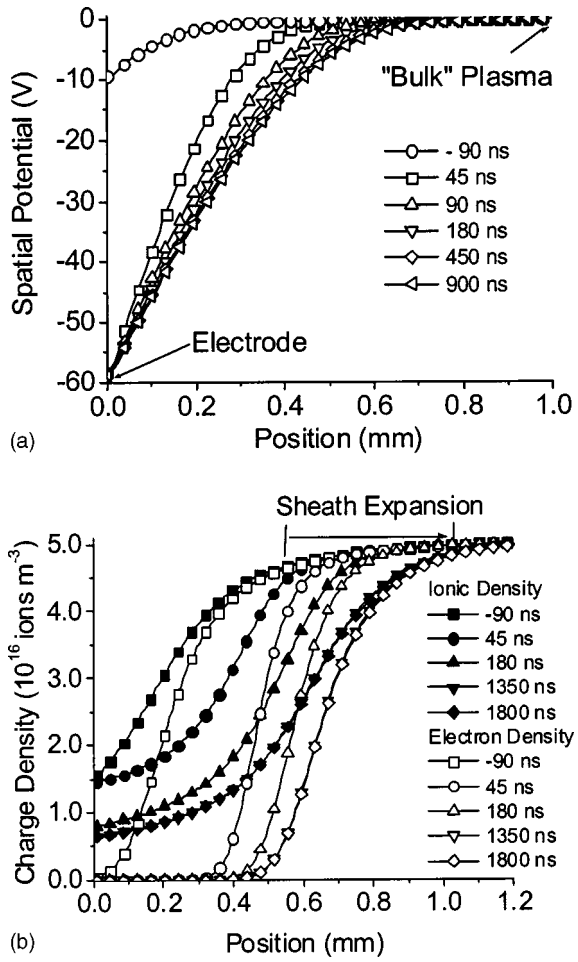

FIG. 1. Spatial and temporal evolution of (a) the electrical potential and (b) the charge density after the application of a 50-V pulse.

$$\frac{\partial x}{\partial t} = u_i , \tag{5b}$$

describe the motion tracer ions under the influence of the electric fields in the sheath. The acceleration and displacement of the ions are solved with Eq. (5a) and Eq. (5b) using the leapfrog algorithm [20] and incrementally increasing time by Δt. The interval of time Δt was chosen in such a manner as to keep the displacement of a tracer particle drifting at a speed of u_{Bohm} from advancing more than one trace cell width. This prevented the draining of the sheath and led to a stable sheath solution.

The ionic density was obtained by employing the ionic continuity condition,

$$\frac{\partial n_i}{\partial t} + \frac{\partial}{\partial x}(n_i u_i) = 0. \tag{6}$$

The density of the jth tracer cell was obtained by imposing a fixed number of ions in any given tracer cell for all times. With this condition, the solution of Eq. (6) takes the following form,

$$n_{ion}^{j}(x,t) = n_{ion}^{j}(x,t-\Delta t)\,\frac{(x^{j+1}-x^{j})|_{t-\Delta t}}{(x^{j+1}-x^{j})|_{t}}. \tag{7}$$

The density of trace cell j at time t is related to the density of the same trace cell at time $t-\Delta t$ and the ratio of the initial cell volume (at time $t-\Delta t$) to the new cell volume (evaluated at time t). After determining the response of the trace ions to the fields and calculating the resulting trace ion density for each cell, the new trace densities used to calculate the densities of the fixed reference points and the procedure described in this section is continually repeated for tens of pulse cycles.

III. SHEATH DYNAMICS

A. Transient sheath evolution

Using the model described in the preceding section, we calculated the evolution of the sheath under the application of a 50-V pulse ($V_{Low}=-60$ V, $V_{High}=-10$ V). Figures 1(a) and 1(b) are the calculated spatial evolution of the sheath's potential and charge density for different times after the electrode is pulsed from V_{High} to V_{Low}. The density of the argon ($m_i=6.68\times10^{-26}$ kg) plasma is set to 5×10^{16} ions m^{-3} and the pulse frequency is 100 kHz with a 50% duty. Two points are illustrated in Figs. 1(a) and 1(b). First is the stability of the sheath after being pulsed, illustrating the ability of the model to predict the sheath's equilibrium structure. The second point illustrated in Figs. 1(a) and 1(b) is the transient nature of the sheath in response to the applied pulse. The ions require a finite time to respond to the transient potential and require some time after the pulse to obtain an equilibrium distribution. For the given plasma conditions, the sheath obtains an equilibrium distribution in a time on the order of 500 ns.

B. Transient ionic flux and energy

Because of the finite response of the ions to the transient potential of the driving electrode, the temporal dependence of the ionic flux and the energy these ions posses when they impact the electrode will become complex functions of time. The manifestation of this temporal dependence of the ionic flux is in the form of displacement currents associated with the restructuring of the sheath to shield the electrode's potential from the bulk of the plasma.

Figures 2(a) illustrates the ionic flux to the electrode as a function of time for the 50-V pulse at 100 kHz (50%). Note the break in the horizontal scale, to illustrate the effects of the transient sheath on the extracted current of the ions. When the electrode is pulsed from V_{High} (-10 V) to V_{Low} (-60 V), the electrons are instantaneously repelled from the electrode, exposing an ionic matrix, as described by Libermann [21]. The exposed ions that are drained from the sheath, to the electrode, during the restructuring of the sheath constitute the displacement currents. As the sheath approaches the equilibrium distribution [Figs. 1(a) and 1(b), for example], the displacement currents decay and the ionic current approaches that of the Bohm current (the product of the Bohm velocity and the ionic density of the bulk plasma), or

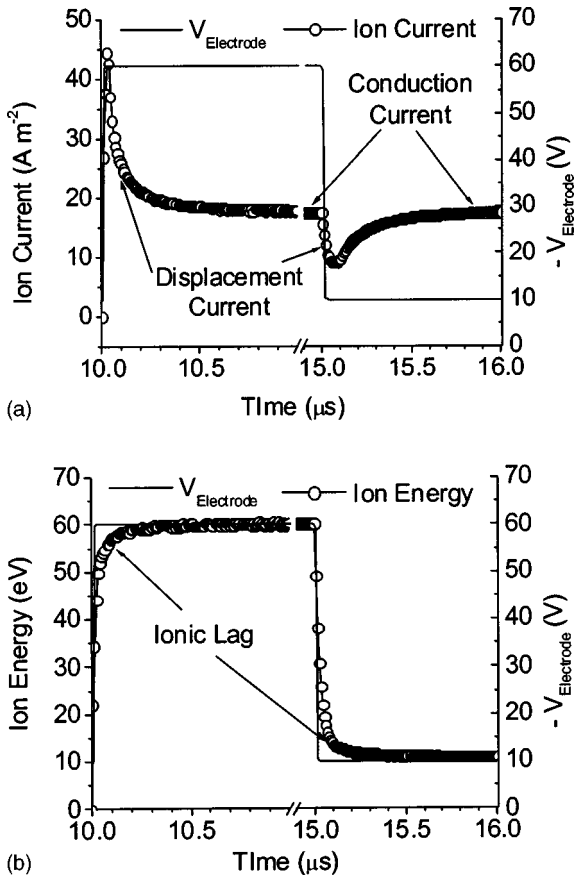

FIG. 2. Temporal evolution of (a) the ionic currents and (b) the ionic energies in response to a 50-V bias pulsed at 100 kHz.

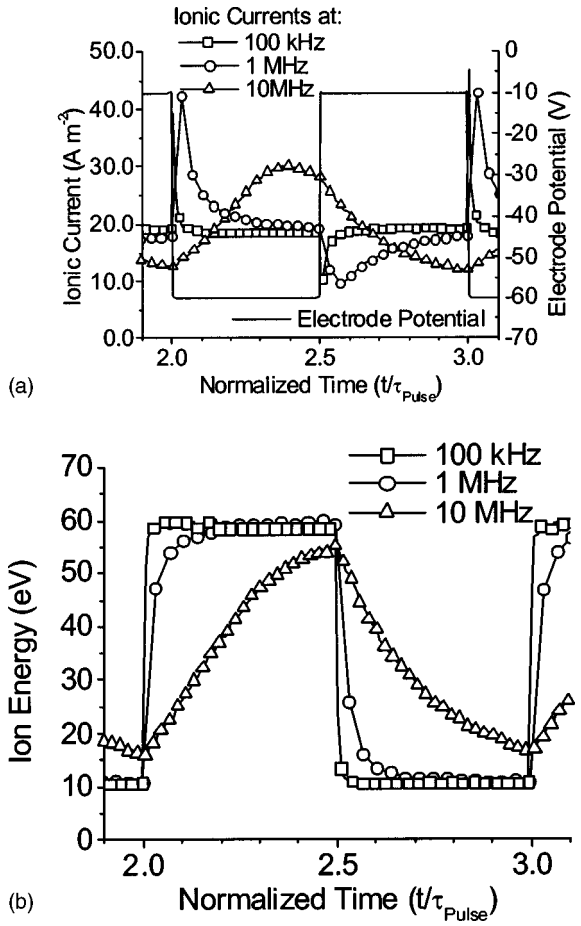

FIG. 3. Evolution of the (a) ionic currents and (b) the ionic energies as functions of normalized time (normalized to the pulse period) for a 100-kHz, 1- and 10-MHz pulse.

conduction current. Approximately 500 ns after the pulse, the ionic current to the electrode is primarily the Bohm current that had diffused from the plasma into the sheath, calculated to be 18.1 Å m^{-2}. Likewise, when the electrode is pulsed from V_{Low} to V_{High}, the electrons instantaneously flow from the plasma into the sheath because of the reduced fields in the sheath, leaving a depleted ''pre-sheath'' region. Conduction current flowing from the bulk plasma will ''fill in'' this depleted region, reducing the current to the electrode until an equilibrium distribution of charge is once again established.

Figure 2(b) illustrates the finite response of the ions to the transient fields in the plasma that arise from the ion's inertia. Again, note the break in the horizontal axis used to highlight the phenomenon of interest. During the initial period after an applied pulse from V_{High} to V_{Low}, the ions in the sheath, close to the electrode, would not obtain a kinetic energy prescribed by the ''new'' voltage drop across the sheath. As time progresses and the ions in the sheath immediately after the pulse are drained to the electrode, subsequent ions that enter the sheath will obtain a kinetic energy prescribed by the potential drop across the sheath. The effect of this ionic inertia is manifested in a ''lag'' between the ionic energy to the electrode and the potential across the sheath. The time scale associated with this inertial effect is on the order of 200 ns. After the electrode is driven from V_{Low} to V_{High}, ions in the sheath have energies prescribed by their position in the sheath before the pulse, which is in excess of the new potential across the sheath. Again, this effect is manifested in the form of a lag between the ion energy and the potential across the sheath.

IV. RESULTS OF TRANSIENT SHEATH DYNAMICS

In this section, we discuss factors that ultimately influence the final energy spectrum of the ions to the electrode. We initially consider the transient time with respect to the time scales of the driving pulse and the impact of these time scales on the resulting energy spectrums. We then consider the factors that influence the transient time scales, in particular, the density of the plasma. Finally we couple the pulsed electrode to the applied pulse (from the ''generator'') by a capacitor and examine the influence of the displacement currents, from the restructuring of the sheath, have on the rate of charge accumulation.

A. Pulsed waveform

The shape of the pulsed waveform, in particular, the frequency of the pulse and the asymmetry of the pulse, will determine the relative impact the transient behavior of the sheath's response will have on the total ion flux and energies.

Figures 3(a) and 3(b) illustrate the ionic flux and the en-

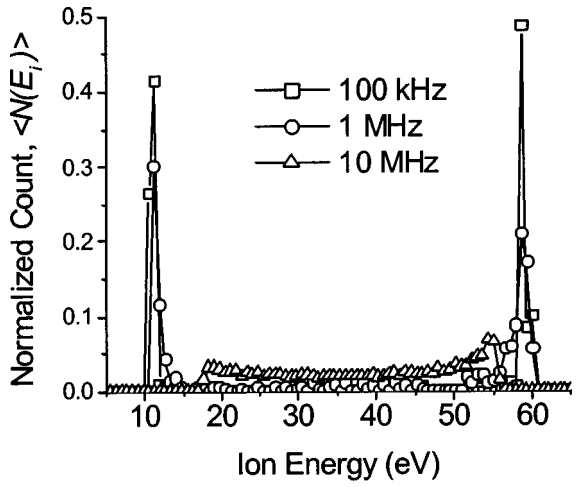

FIG. 4. The calculated energy spectrum of the ions to an electrode pulsed at 100 kHz, 1, and 10 MHz.

ergy of the flux to the electrode as functions of normalized time for a 50-V pulse at 100 kHz (50%), 1 MHz (50%) and 10 MHz (50%). The density of the argon plasma is 5×10^{16} ions m^{-3}. The period of 100-kHz pulse, 10 μs, is large compared to the time for the sheath to undergo restructuring (on the order of 0.5 μs). As a result, only a small percentage of the extracted current is in the form of displacement currents. The resulting energy of the ions extracted from the plasma [Fig. 2(b)] for the 100-kHz case is predominately the energy difference between the plasma (defined as 0 V) and the electrode's potential (either V_{High} or V_{Low}).

For the 1-MHz case, the period of the pulse (1 μs) is comparable to the time the sheath takes to reach an equilibrium distribution. The ionic flux to the electrode is dominantly in the form of displacement currents [Fig. 3(a)]. Ionic inertial effects are manifested more clearly in the energy of the ions extracted to the electrode for the 1-MHz pulse [Fig. 3(b)].

The final case, 10 MHz with a period of 100 ns, illustrates the behavior of the sheath when the time scales of the pulse become smaller than the time scales of the sheath's response. Like the 1-MHz case, the current to the electrode is in the form of a displacement current, but unlike the 1-MHz case, the sheath never obtains equilibrium. As a result of the sheath's inability to reach an equilibrium distribution, the magnitude of the displacement currents become reduced. Likewise, ions in the sheath during a pulse are never completely drained to the electrode, preventing the ions from obtaining a kinetic energy as prescribed by the potential of the sheath.

The ionic inertial and ionic displacement phenomenon, are taken in combination when considering the ion energy spectrum. For our discussion we obtain the ion energy spectrum by calculating the normalized ion count, $\langle N(E_i)\rangle$, possessing energies between $E_i\pm\Delta E/2$, as prescribed by

$$\langle N(E_i)\rangle\big|_{E_i-(\Delta E/2)}^{E_i+(\Delta E/2)}=\frac{\int_{t_1}^{t_2}j_{ion}(t)dt}{\int_{Period}j_{ion}(t)dt}. \tag{8}$$

The bounds on the integral in the numerator in Eq. (8), t_1 and t_2, correspond to the times the ionic current to the electrodes have energies in the domain of $E_i\pm\Delta E/2$. The normalized ion count is then calculated and plotted as a function of E_i. Figure 4 is the resulting energy spectrum of the ions extracted to the electrode for the three pulse frequencies discussed (100 kHz, 1, and 10 MHz), using a ΔE of 0.5 eV. The 100-kHz distribution is bimodal, displaying two sharp peaks centered about 10 and 60 eV, respectively. This is expected because the majority of the ions possess an energy as prescribed by the potential across the sheath. A slight asymmetry is observed for the 100-kHz spectrum caused by a small contribution of the displacement currents to the total currents per cycle. The sharp bimodal distribution was also predicted using the quasistatic treatment of the sheath's response to the transient pulse, as discussed in previous studies [5,14,15]. Only slight discrepancies arise from the small but finite contribution of the transient effects on the ionic flux. Factoring in these displacement currents, there are slightly more high-energy ions ($\sim$60 eV) than low-energy ions ($\sim$10 eV). The 1-MHz spectrum is also bimodal in nature, but the two peaks are broadened by the increased role ionic inertia plays in the energies of the total ionic flux to the electrode, per cycle. Finally, the 10-MHz spectrum is broad, with only a small peaks in the high and low extreme ends of the energy spectrum.

The degree of asymmetry of the pulse can be changed by changing the duty of the pulse. Figures 5(a), 5(b), and 5(c) illustrate the effect of increasing the pulse duty from 50% to 90% for the 100 kHz, 1-, and 10-MHz pulses. The duty of the 100-kHz pulse is changed from 50% to 90% in Fig. 5(a). As a result of the change in the duty, the 10-eV peak decreases and 60-eV peak increases. This is essentially the same behavior as predicted from calculations using a quasistatic treatment of the sheath's response to the transient fields [5,14,15]. The effect of varying the duty of the 1-MHz pulse is shown in Fig. 5(b). Unlike the 100 kHz, the time scales of the pulse are comparable to the sheath's time scales. With an increase in the duty, from 50% to 90%, the time the electrode is pulsed to V_{High} is reduced from 500 to 100 ns, insufficient time is given for the ions to achieve an equilibrium configuration [see Figs. 2(b) and 3(b)]. As a result, the bimodal nature of the energy spectrum exhibited for the 50% duty is eliminated when the duty is set to 90%. The energy spectrum of the 10 MHz, Fig. 5(c), further illustrates the impact of transient response of the sheath on the energy spectrum of the ions with a change in the pulse duty. The bimodal nature of the distribution is suppressed at 50% duty, as discussed previously in terms of the sheath's response time to transient potentials. With an increase of the duty and subsequent reduction of allotted time for the sheath's response to the applied V_{High}, the energy distribution narrows towards the high-energy end of the spectrum. At 90% duty, the spread of the energy is less than 20 eV. The quasistatic treatment used to describe the sheath's response to lower frequency pulses ($\leqslant$100 kHz) [5,13–15] would not be able to predict the energy spectrum of the 1- and 10-MHz cases calculated in this study.

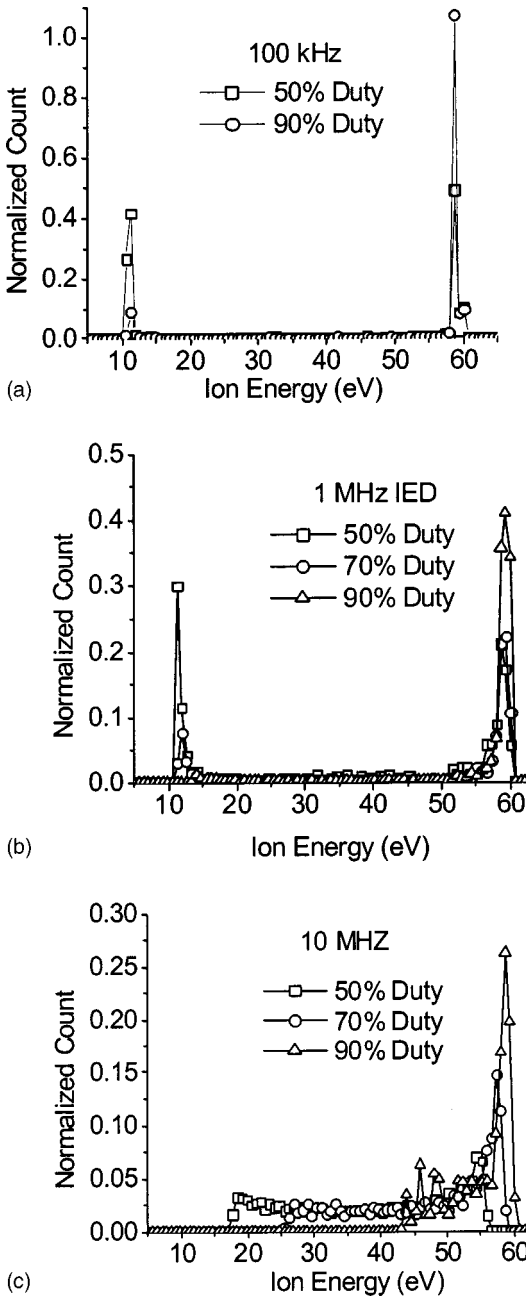

FIG. 5. Energy spectrum of ions extracted from the plasma to an electrode driven at (a) 100 kHz, (b) 1 MHz, and (c) 10 MHz at various duties (50%, 70%, and 90%).

B. Plasma density

The sheath is a non-neutral space charge that establishes the potential difference between the electrode and the plasma, shielding the plasma from the potential of the electrode. The length scales associated with the screening of potentials in the plasma are typically discussed in terms of the Debye length, prescribed in Eq. (1). The effectiveness of the plasma to screen the potential is proportional to the square root of the plasma's density, n_0. As a result of the screening's dependence on the density of the plasma, it is expected that the transient nature, in particular, the amount of displacement current and the time the sheath requires to undergo restructuring, will depend on the plasma's density.

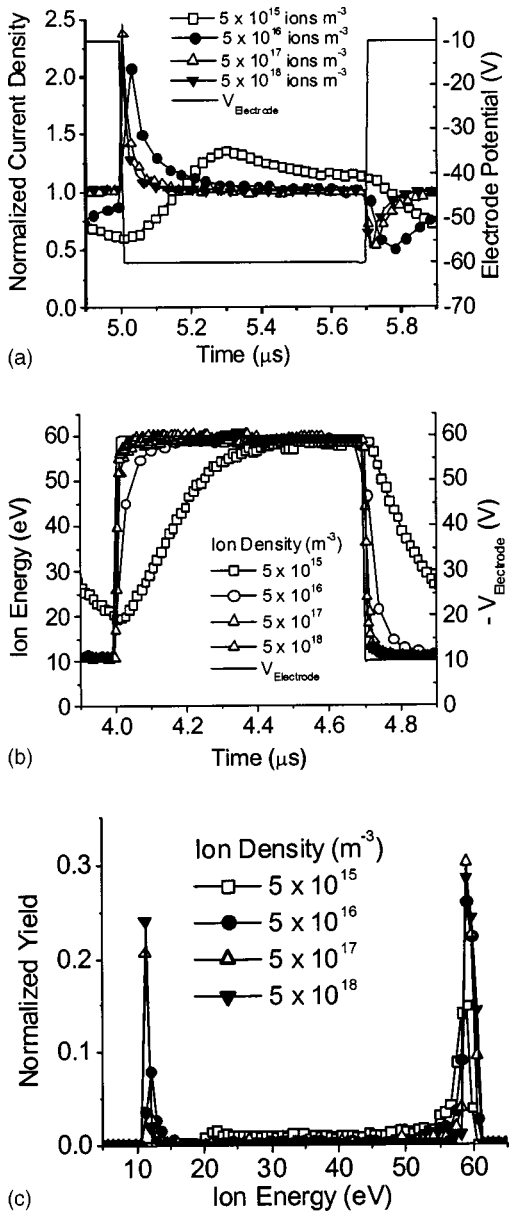

FIG. 6. The calculated evolution of the (a) ionic currents and (b) ionic energies and (c) the resulting ion energy spectrum for various plasma densities. [$V_{\mathrm{Pulse}}=50$ V at 1 MHz (70%).]

The impact of the plasma's density on the extracted charge from the plasma, to an electrode driven at -50 V at 1 MHz with a 70% duty, is plotted in Fig. (6). In Fig. 6(a), the current is normalized to the Bohm current from the plasma. The densities considered range from 5×10^{15} to 5×10^{18} ions m^{-3}. Clearly, as the density increases, the time required for the sheath to reach an equilibrium distribution decreases (gauged by the time scales of the transient currents and energies). The decrease in the transition time with an increase in density is due to a decreased sheath width and ultimately shortened times for the ions to transit the sheath. The behavior of the low density (5×10^{15} ions m^{-3}) sheath's response to the pulse at 1 MHz is analogous to the behavior of the 5×10^{16} ions m^{-3} sheath's response at 10 MHz. For both cases, the ions do not have enough time to reach an

equilibrium distribution. The ion energy spectrum for the four densities are plotted in Fig. 6(c) using the information in Figs. 6(a) and 6(b).

C. Capacitive coupling

The previous discussions had focused on the response of the plasma to an asymmetrically pulsed bias applied to a conducting electrode. In this section, the electrode is coupled to the applied pulse through a coupling capacitor. The coupling capacitor is typically used when a dielectric material is placed on an electrode, and is chosen to prevent deleterious potentials from being induced across the dielectric. Because of the capacitive coupling, charge extracted from the plasma will accumulate on the electrode and a potential will be induced across the capacitor. The rate of charge accumulation, the subsequent potential evolution of the surface and the impact of charge accumulation on the currents and energies of the charged particles extracted from the plasma had been the subject of previous studies [5,13–15]. Of particular interest in this discussion is the increasing importance of the displacement charge on the rates of charge accumulation.

To account for the effects of charge accumulation on the potential of the capacitively coupled electrode, the boundary condition as prescribed by Eq. (4a) is modified through the modification of the dc term A_0 in Eq. (4b). The modification of A_0 is given by

$$A_0(t)=\frac{e}{\tau}[V_{Low}\tau_{Low}+V_{High}\tau_{High}]+\frac{e}{C}Q(t). \quad (4b')$$

In Eq. (4b′), C is the blocking capacitance, and $Q(t)$ is the sum of the ionic and electronic charge to the electrode and is a function of time. Equation (4b′) assumes that the impedance of the blocking capacitor is less than the total impedance offered to the pulse through the electrode's sheath, the bulk plasma and the sheath between the plasma to the grounded chamber wall. This assumption of the small impedance of the blocking capacitor with respect to the (capacitive) impedance of the sheath-plasma-sheath system allows us to treat the voltage drop across the capacitor as being only due to the accumulated charge. An order of magnitude calculation of the sheath's capacitance is obtained by considering the charge in the sheath to be on the order of 1×10^{16} ions m^3 for a 5×10^{16} ions m^{-3} bulk plasma. Using the area of 0.031 m^2 (0.2 m or 8-inch diameter), a sheath width of 1 mm, and a voltage of 100 V, the sheath's capacitance is approximated to be on the order of 0.1 nF. Considering the series combination of the plasma's capacitance and the plasma-wall capacitance, blocking capacitances on the order of 1 nF satisfy the low impedance approximations required for the use of Eq. (4b′).

For the following discussion, a 200-mm electrode is driven by a 50-V pulse at 1 MHz and 70% duty through a coupling capacitor. The density of the plasma is 5×10^{16} ions m^{-3}. The calculated influence of the presence of a 5-nF blocking capacitor on the total current, the electrode potential and the resulting energy spectrum are shown in Figs. 7(a), 7(b), and 7(c). For each of the cases, a comparison

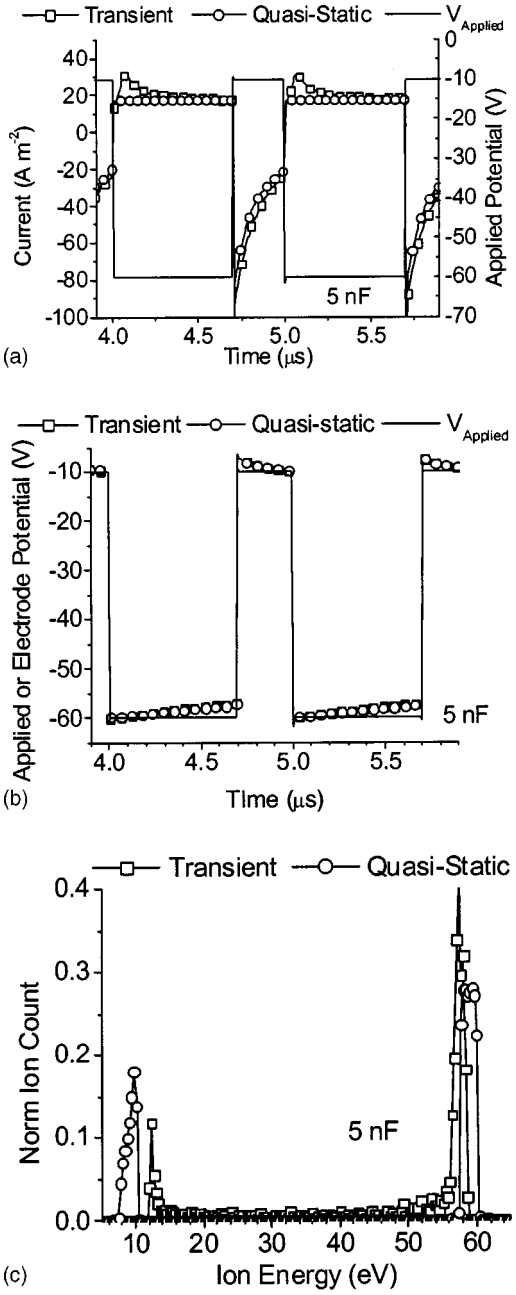

FIG. 7. A comparison of the temporal evolution of (a) the total currents and (b) the electrode potential to an electrode as predicted by the quasistatic and transient treatments of the sheath. The resulting (c) energy spectrum of the ions obtained from the (a) currents and (b) energies. [$V_{Pulse}=50$ V at 1 MHz (70%), $C_{Block}=5$ nF.]

is made between the transient treatment discussed in this study and the quasistatic treatment discussed in other studies [5,13–15]. Figure 7(a) plots the combined ionic (positive) and electronic (negative) currents as predicted by both the transient model of the sheath and the quasistatic treatment of the sheath. The transient currents are mostly in the combined form of displacement and conduction currents, as discussed above, while the quasistatic currents are just the dc conduction currents through the sheath. Figure 7(b) illustrates the evolution of the electrode's potential in time as a result of the

current extracted from the sheath as calculated in Fig. 7(a). The excess displacement charge to the electrode induces a potential difference on the order of 5 V, not quite discernable in Fig. 7(b). The resulting ion energy spectrums for the two treatments are plotted in Fig. 7(c), where there is some noticeable difference between the two treatments. The slight narrowing of the energy spectrum obtained by considering the transient nature of the sheath is caused by the lag of the ions to changes in the electrode's potential. The differences in the peak amplitudes is a result of the excess displacement current predicted by the transient treatment.

The same consideration is given for a 500-pF coupling capacitor in Figs. 8(a), 8(b), and 8(c). Figure 8(a) plots the total currents to the electrode (ionic and electronic), obtained using the transient and quasistatic sheath treatments. The evolution of the currents are similar to the evolution of the currents for the 5-nF case, with the exception that the currents go to zero when the 500-pF capacitor is pulsed to V_{High}. For the 500-pF case at V_{High}, sufficient electronic charge is extracted to bring the surface to the floating potential (an equilibrium potential where the ionic flux from the plasma equals the electronic flux from the plasma). Displacement currents are observed to play a more noticeable role in the evolution of the electrode's potential as illustrated in Fig. 8(b). The resulting ion energy distributions predicted by the two treatments are plotted in Fig. 8(c). Clearly, the distribution predicted by the transient treatment is considerably narrower than the distribution predicted by the quasistatic treatment. This narrowing of the distribution results not only from the ionic lag, but the increased role the displacement charge plays in the evolution of the potential's surface.

V. SUMMARY AND CONCLUSION

A model was used to predict the behavior of a sheath, in particular, the restructuring of the sheath and the ionic response to an asymmetrically pulsed dc bias. The model and procedures used to solve for the sheath's evolution in time and space were described. The spatial and temporal evolution of the sheath's charge and potential were plotted to illustrate the time scales associated with the sheaths response to the pulse. Temporal evolution of the ionic current demonstrated the effect the sheath's restructuring had on the currents to the electrode. The current was composed of both a displacement and conduction component. The dependence of the ionic energy in time also illustrated the lag between the applied potential and the kinetic energy the ions obtain. This ionic lag was discussed in terms of the ion's motion in the sheath prior to the application of the transient bias. The lag was the manifestation of the ionic finite time to cross the sheath. Ion energy distributions were obtained using the calculated temporal response of the ionic current and energies. The transient behavior influenced the energy distributions in two ways. First, displacement currents changed the relative percentages of the flux to the electrode at any given time during a cycle. Second, the ionic lag caused a smearing, or broadening, of the high- and low-energy peaks and a narrowing of the spectrum, in general.

Discussion was given in terms of the relative impact of these transient effects with respect to the total ion flux extracted from the plasma, per cycle. Specifically, time scales of the pulse were discussed with respect to the time scales of the transient response of the sheath. For a bulk density of 5×10^{16} ions m^{-3}, the energy spectrum of the ions from the plasma driven by the low frequency pulse (100 kHz) was essentially unaffected by the transient effects while the spectrum of the ions driven by both the 1 and 10 MHz were significantly influenced by the transient behavior of the sheath's response to the pulse. Time scales of the sheath's response were then discussed in terms of the plasma's den-

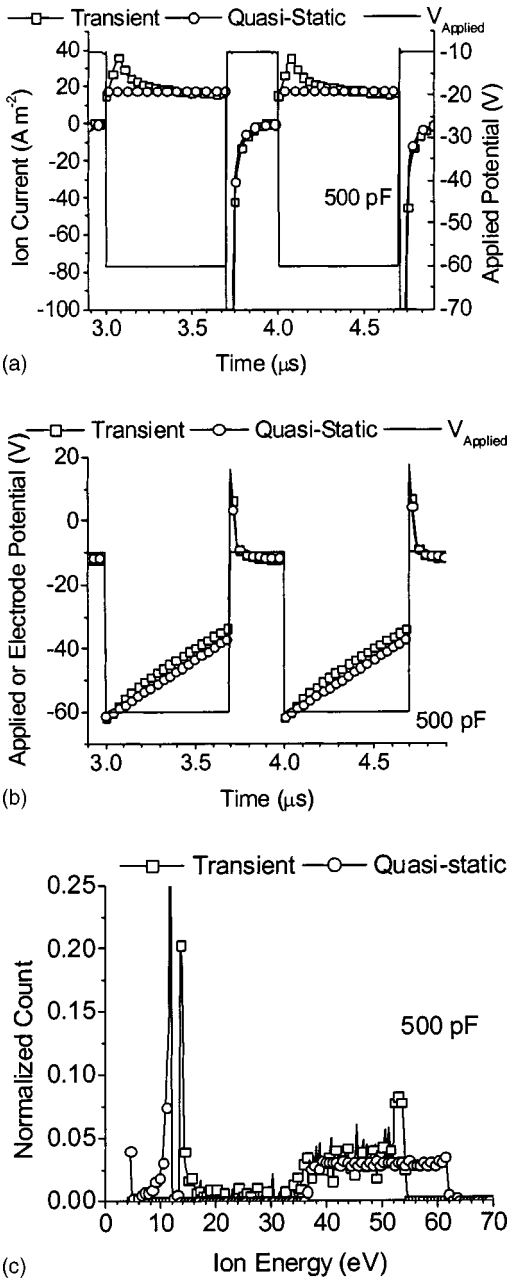

FIG. 8. A comparison of the temporal evolution of (a) the total currents and (b) the electrode potential to an electrode as predicted by the quasistatic and transient treatments of the sheath. The resulting (c) energy spectrum of the ions obtained from the (a) currents and (b) energies. [$V_{\mathrm{Pulse}}=50$ V at 1 MHz (70%), $C_{\mathrm{Block}}=500$ pF.]

sity. With an increasing availability of charge, corresponding to an increasing effectiveness to shield the bulk plasma for the electrode's fields, there was a decreasing time for the sheath to undergo restructuring.

Finally, the effect of coupling the applied pulse to the electrode, was discussed. The evolution of the charge from the plasma and the energy of the ions to the electrode were calculated for two capacitive couplings using the transient sheath treatment (discussed here) and a quasistatic sheath treatment [5,13–15]. Comparison of the currents and energies were made between the two treatments. For the large capacitance case (5 nF) little difference is observed between the two cases, while a significant difference is observed between the two treatments for the 500-pF case. Theses differences are primarily due to the increasing contribution of the displacement charge on the induced potential across the charging capacitor.

The transient model is used to predict the sheath's transient behavior to an asymmetrically pulsed bias that was neglected in the quasistatic treatment of the sheath in previous studies. Comparison of cases employing low frequency ($\leqslant$100 kHz) or large capacitive coupling suggest that the quasistatic treatment can be used as a good approximation of the sheaths behavior. On the other hand, as the timescales approach those associated with the response of the ions to the transient fields (high frequency limit) or the role of displacement currents cause a significant induced potential across a blocking capacitor (small capacitance limit) the quasistatic treatment becomes inaccurate and the transient treatment described here is required.

ACKNOWLEDGMENTS

The authors would like to thank J. Juneja for his comments on the manuscript. E. B. was financially supported through the Intel Foundation and by the Center for Advanced Interconnect Technologies (CAIST) at RPI.

[1] N. W. Cheung, Nucl. Instrum. Methods Phys. Res. B **55**, 811 (1991).
[2] J. R. Conrad and T. J. Castagna, Bull. Am. Phys. Soc. **31**, 1479 (1986).
[3] S.-B. Wang and A. E. Wendt, J. Vac. Sci. Technol. A **19**, 2425 (2001).
[4] E. Collard, C. Lejuene, J. Grandchamp, J. P. Gilles, and P. Scheiblin, Thin Solid Films **193**, 100 (1990).
[5] E. V. Barnat, T.-M. Lu, and J. Little, J. Appl. Phys. **990**, 4946 (2001).
[6] H. Hirayama, H. Okamoto, and K. Takayanagi, Phys. Rev. B **60**, 14 260 (1999).
[7] E. A. Edelberg, A. Perry, N. Benjamin, and E. S. Aydil, J. Vac. Sci. Technol. A **17**, 506 (1999).
[8] N. Mizutani and T. Hayashi, J. Vac. Sci. Technol. A **19**, 1298 (2001).
[9] M. A. Liberman, IEEE Trans. Plasma Sci. **16**, 638 (1988).
[10] A. Metze, D. W. Ernie, and H. J. Oskam, J. Appl. Phys. **60**, 3081 (1986).
[11] T. Panagopoulos and D. J. Economou, J. Appl. Phys. **85**, 3435 (1999).
[12] M. A. Sobolewski, J. K. Olthoff, and Y. Wang, J. Appl. Phys. **85**, 8 (1999).
[13] E. V. Barnat and T.-M. Lu, J. Vac. Sci. Technol. A **17**, 3322 (1999).
[14] E. V. Barnat and T.-M. Lu, J. Appl. Phys. **90**, 5898 (2001).
[15] E. V. Barnat and T.-M. Lu (unpublished).
[16] M. Widner, I. Alexeff, and W. D. Jones, Phys. Fluids **13**, 2532 (1970).
[17] G. A. Emmert, J. Appl. Phys. **71**, 113 (1992).
[18] C. K. Birdsall and A. B. Langdon, *Plasma Physics Via Computer Simulation* (IOP publishing Ltd., Bristol, 1991), Chap. 2, p. 19.
[19] R. W. Hockney and J. W. Eastwood, *Computer Simulation Using Particles* (Adam Hilger, New York, 1988), p. 185.
[20] C. K. Birdsall, *Plasma Physics via Computer Simulation* (McGraw-Hill, New York, 1985), p. 12.
[21] M. A. Liberman and A. J. Lichtenberg, *Principles of Plasma Discharges and Materials Processing* (Wiley, New York, 1994), Chap. 16, p. 528.